

Systematic Variations in Lava Flow Morphology Along the North and South Rift Zones of Axial Seamount

Jennifer Paduan¹, David Clague¹, David Caress¹, Morgane Le Saout², and Brian Dreyer³

¹Monterey Bay Aquarium Research Institute

²GEOMAR

³University of California Santa Cruz

November 22, 2022

Abstract

Meter-scale AUV mapping of 85-km of the summit and rift zones of Axial Seamount shows systematic variation in morphology of the lava flows with depth and distance from the caldera. ROV sampling reveals flow age and chemistry variations. Each rift zone has a steady downward slope of $\sim 2^\circ$ outside the caldera. In the caldera and first few km down the rift zones, flows are predominantly channelized sheet flows with collapses along the channels. Mid-rift, drained inflated hummocky flows consisting of complex mounds with tumuli and lava lakes, and narrow ridges of hummocky mounds become common. On the axis of the south rift, the first cones with craters occur 3.2 km from the caldera at 1600 m depth, and broad inflated hummocky flows emplaced through complex lava tubes first appear 6 km down-rift at 1715 m. On the north rift, similar cones and complex flows appear at 10.5 km down-rift at 1725 m depth. The historical flows exemplify this variation: on the upper south rift as channelized sheet flows in 1998 and 2011 erupted from fissures that extended 6.5 km down-rift; on the middle north rift, inflated hummocky flows up to 126 m thick erupted in 2015 from fissures 17.5 km from the caldera; and on the distal south rift, a narrow ridge of coalesced hummocks 160 m tall formed during the 2011 eruption. Older and older lavas remain exposed at greater distances from the more active summit and upper rift zones. Deep on the rift zones, stellate and steep cones with smooth talus slopes occur that did not feed expansive flows, despite being constructed of hotter, less viscous, near-primary magmas. These cones are first observed on both rift zones at 1800 m depth and 18 km from the caldera. Deeper still, emanating from both distal rift axes beginning ~ 30 km from the caldera, lie voluminous inflated sheet and inflated hummocky flows 30 to 135 m thick with combined area of over 150 km². The plagioclase-phyric voluminous flows on the south rift erupted ~ 1250 years ago, and the aphyric ones on the north rift $\sim 13,000$ years ago. Eruption rate is the most likely cause of the flow morphology changes since estimated magma viscosity does not correlate with flow morphology. Lateral transport through long dikes would slow magma delivery unless dike widths are large. The near-primary magmas may have risen through narrow conduits from the mantle to the distal rifts.



1. SUBMARINE RIFT ZONE FLOW MORPHOLOGY VARIATIONS

Mapping of the summit and rift zones of Axial Seamount shows variations in the morphology of lava flows with depth and distance from the caldera. The variations offer insights into the plumbing of the volcano.

[VIDEO] <https://www.youtube.com/embed/Hq-XERexZL4?rel=0&fs=1&modestbranding=1&rel=0&showinfo=0>

Fig. 1.1) Video showing how we use AUVs and ROVs to map and sample the lava flows.

The historical flows, which erupted from dikes that propagated from the summit caldera down the axes of the rift zones, and the older lavas that remain exposed at greater distances from the more active summit and upper rift zones, all follow this pattern.

More about our vehicles:

[MBARI ROV Doc Ricketts](https://www.mbari.org/at-sea/vehicles/remotely-operated-vehicles/rov-docricketts-specifications-2/) (https://www.mbari.org/at-sea/vehicles/remotely-operated-vehicles/rov-docricketts-specifications-2/)

[MBARI Mapping AUVs](https://www.mbari.org/at-sea/vehicles/autonomous-underwater-vehicles/seafloor-mapping-auv/) (https://www.mbari.org/at-sea/vehicles/autonomous-underwater-vehicles/seafloor-mapping-auv/)

[VIDEO] <https://www.youtube.com/embed/sRQ8bbA3FW8?fs=1&modestbranding=1&rel=0&showinfo=0?rel=0>

Fig. 1.2) Video of the launch of an MBARI Mapping AUV from the R/V Rachel Carson.

2. AXIAL SEAMOUNT MAP

Axial Seamount is a hot-spot volcano interacting with the Juan de Fuca Ridge in the NE Pacific. Its summit and rift zones have been mapped at 1-m resolution, revealing the character of eruptions that have occurred recently and in the past. Here we focus on the rift zones.

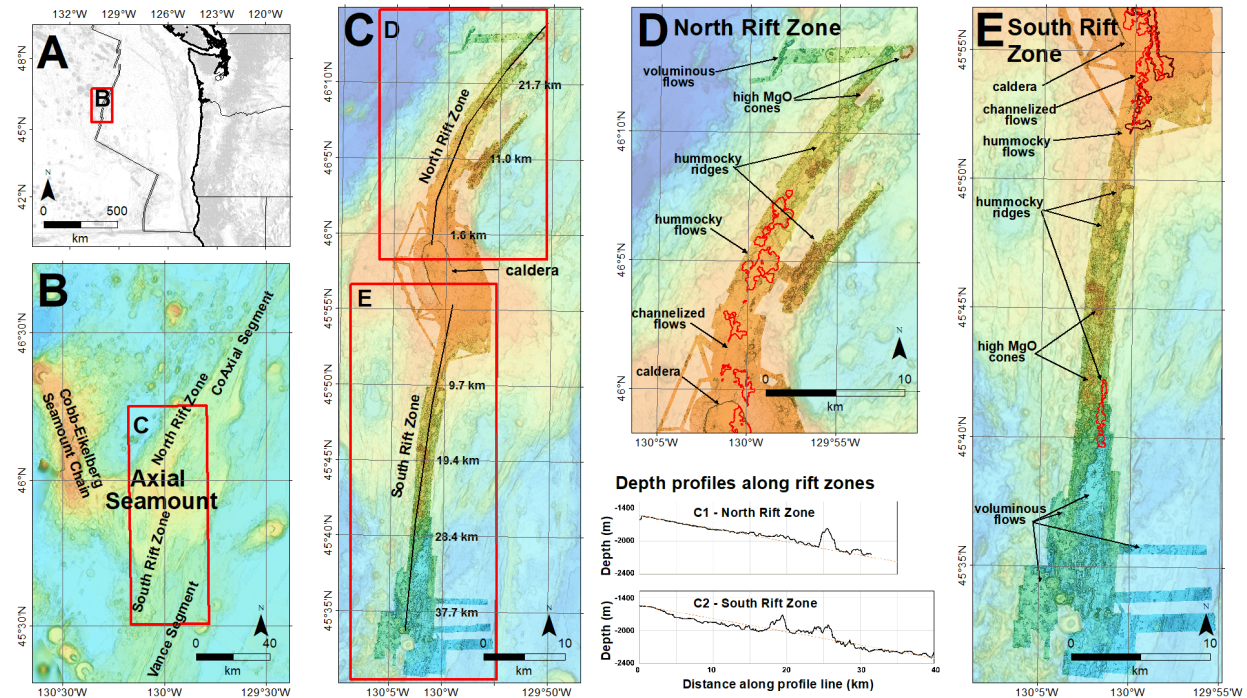


Fig. 2) Maps of Axial Seamount. AUV bathymetry at 1-m resolution is superimposed over slightly faded ship-collected bathymetry.

A: Location of Axial Seamount (in red box) on the Juan de Fuca spreading ridge.

B: Location of Axial relative to the neighboring segments of the Juan de Fuca Ridge and the Cobb-Eikelberg Seamount Chain.

C: 85 km of the north and south rift zones and the summit caldera have been mapped by AUV at 1-m resolution. Black lines (labeled at lines of latitude with distances along the lines from the 8x3 km caldera) are the lines for the depth profiles shown in the plots C1 and C2 for the north and south rift zones, respectively.

C1 and C2: Depth profiles with distance down the axes of the north (C1) and south (C2) rift zones are the black lines. For reference, lines with 2% slope are the dashed orange lines.

D: AUV-mapped coverage of the north rift zone. Examples of features examined in this poster are indicated with arrows. The 2015 flows are outlined in red after Clague et al. (2017).

E: AUV-mapped coverage of the south rift zone. Examples of features examined in this poster are indicated and the 1998 and 2011 flows are outlined in darker reds after Clague et al. (2017).

3. UPPER AND MIDDLE RIFT ZONES: 3A) CHANNELIZED AND 3B) INFLATED HUMMOCKY FLOWS

3A. Upper rift zone flows are predominantly channelized sheet flows with collapses along the channels.

On the upper south rift, in 1998 and 2011 channelized sheet flows erupted as far as 6.5 km from the caldera from fissures that extended further down-rift (Chadwick et al., 2013; Caress et al., 2012). In 2015, channelized flows erupted from en echelon fissures on the upper north rift (Chadwick et al., 2016).

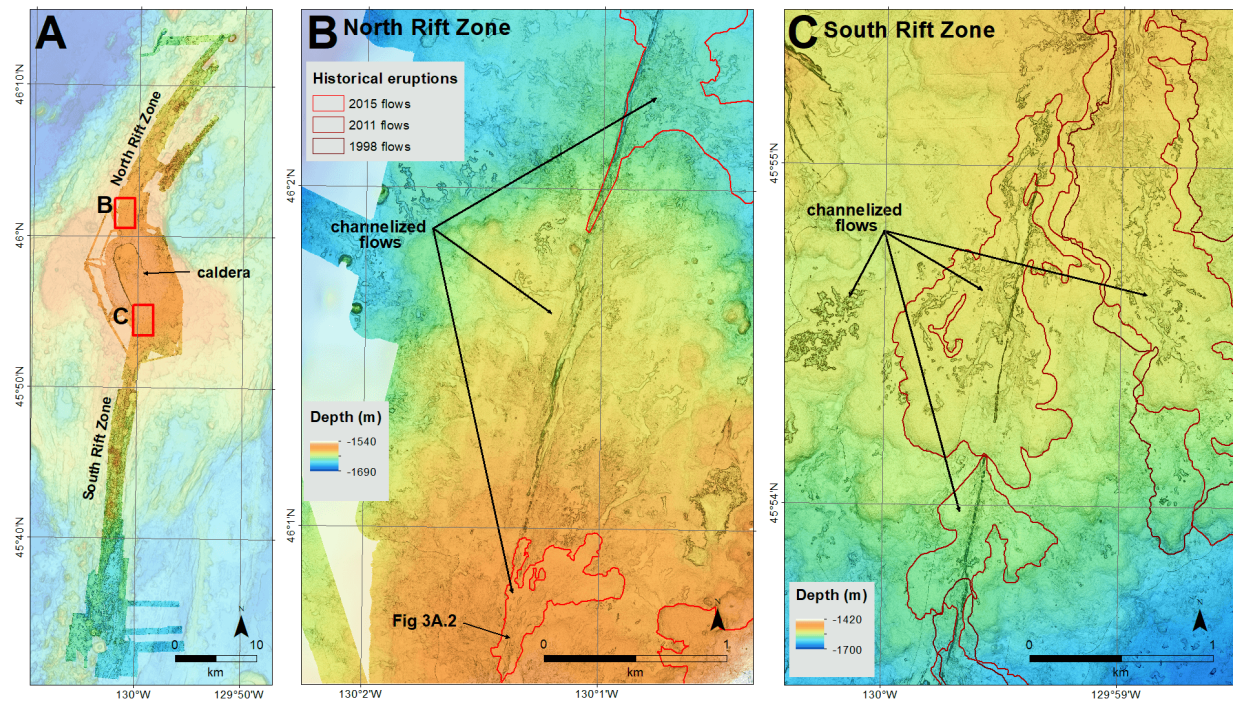


Fig. 3A.1) Maps pointing to some of the channelized flows on the upper rift zones. Location of the ROV dive footage in Fig. 3A.2 is indicated in map B.

[VIDEO] <https://www.youtube.com/embed/OxJVNBqGbbk?rel=0&fs=1&modestbranding=1&rel=0&showinfo=0>

Fig. 3A.2) Video illustrating how channelized flows evolve, and showing the lava pillars that often remain. Location shown in Fig. 3A.1, map B.

3B. On the middle rift zones, inflated hummocky flows become common

On the axis of the south rift, the first cones with craters occur 3.2 km from the caldera at 1600 m depth. Complex inflated hummocky flows first appear 6 km down-rift at 1715 m, as broad, flat-topped structures composed of multiple hummocks, with collapses, rimmed lava lakes, and tumuli on their summits (e.g., Fig. 3B.2). On the north rift, similar cones and complex hummocks appear at 10.5 km down-rift at 1725 m depth.

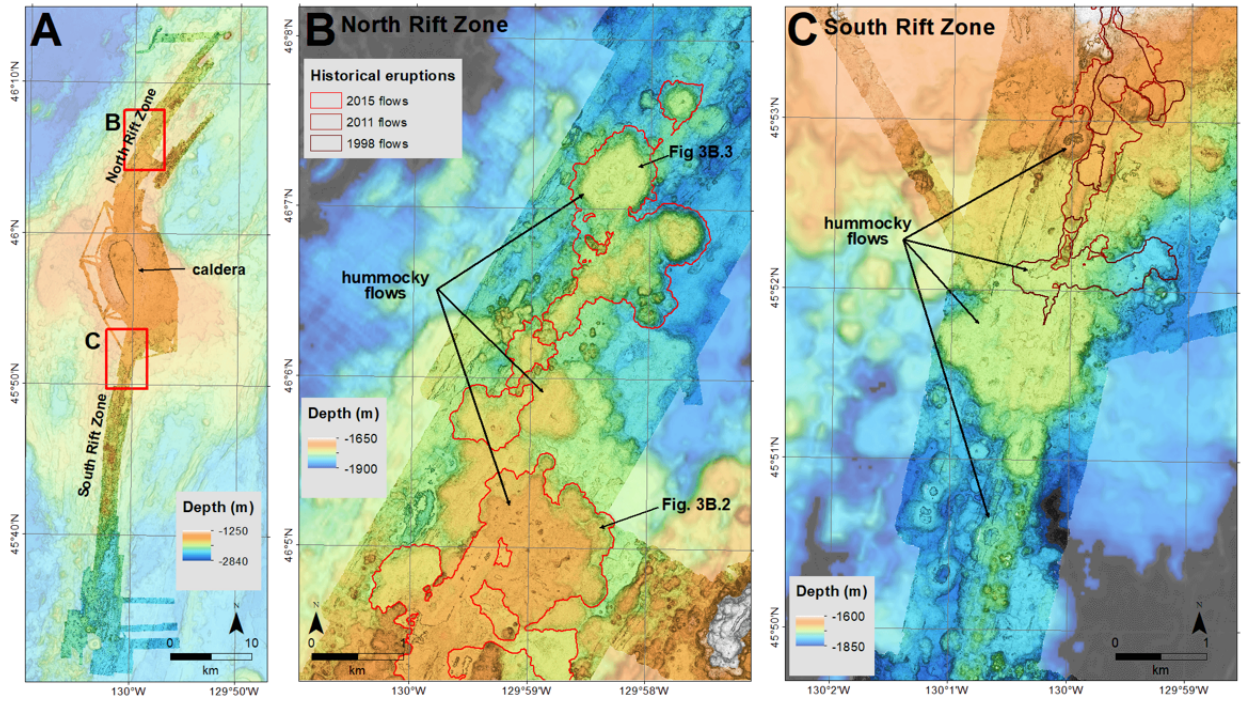


Fig. 3B.1) Maps pointing to some of the inflated hummocky flows on the middle rift zones. Location of hummocks in the following figures are indicated in map B; they were both over 60 m thick (Chadwick et al, 2016).

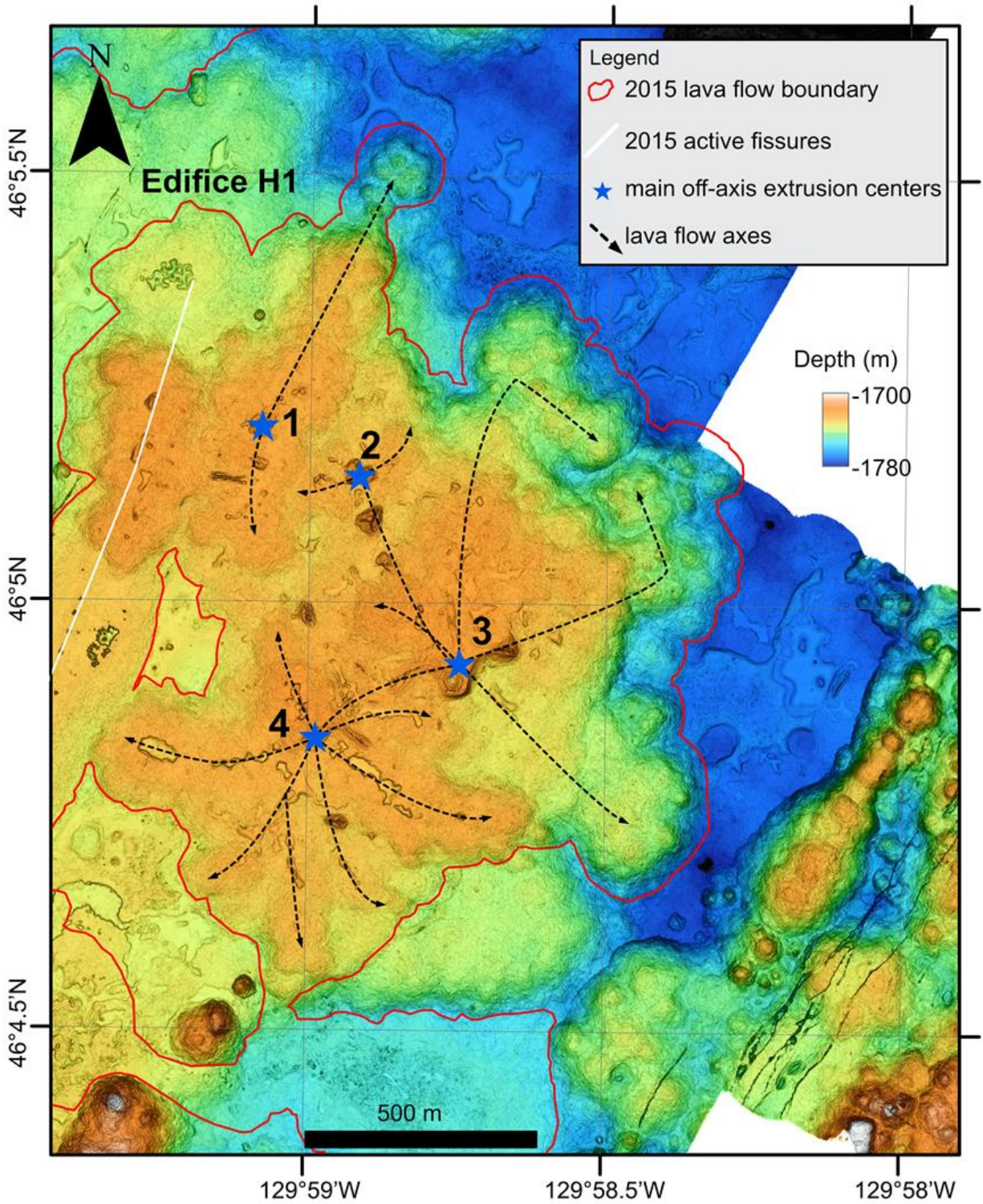


Fig. 3B.2) Inflated hummocky flows expand as lava travels from the fissure (white line) through molten interior pathways (dashed lines), which may emanate from extrusion centers (blue stars) far from the fissures, as tracked by impulsive sounds recorded during the 2015 eruption (Le Saout et al., 2020). Location of this hummock is shown in Fig. 3B.1, map B.

[VIDEO] <https://www.youtube.com/embed/EJu8gt6NNes?rel=0&fs=1&modestbranding=1&rel=0&showinfo=0>

Fig. 3B.3) ROV video of a traverse of the flow front and across the summit lava lake of one of the 2015 inflated hummocks (location shown in Fig. 3B.1). The fluid basaltic lava created smooth, elongate pillows. The interior of the hummock was still cooling and hydrothermal fluids were venting through 0.3 m high chimneys a year later.

4. DEEP RIFT ZONES: 4A) STEEP RIDGES, 4B) HIGH-MGO CONES, AND 4C) VOLUMINOUS FLOWS

4A. On the middle rift zones, steep ridges of coalesced hummocky flows become common.

For long distances, especially on the south rift zone, narrow ridges of steep hummocky flows lie parallel with the rift zone axes. During the 2011 eruption, steep hummocks of elongate basaltic pillow lavas formed 18.5 km down-rift of the upper south rift zone flows (Caress et al., 2012). Older andesite flows built larger hummocks on the north rift. Molten cores allowed hummocks to coalesce and some to grow off-strike of the fissure (e.g., Yeo et al., 2013).

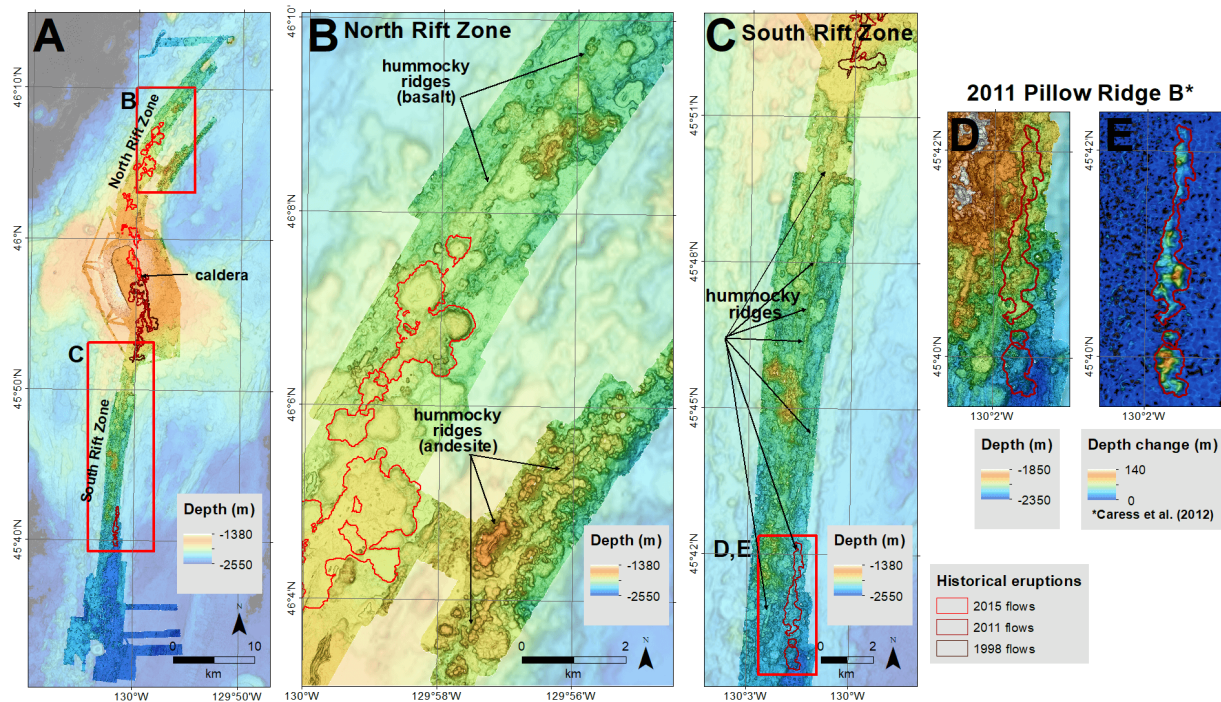


Fig 4A.1) Maps of steep hummocky ridges on the middle and deep rift zones. For more on the andesite cones, see poster V040-0019.

D, E: Ridge of coalesced hummocky flows up to 137 m thick that erupted in 2011 deep on the south rift zone (location in map C). It was discovered by differencing pre- and post-eruption ship-collected bathymetry (map E; Caress et al., 2012) and has now been mapped with the AUV (map D).

[VIDEO] <https://www.youtube.com/embed/aVNG5M4C2Y0?rel=0&fs=1&modestbranding=1&rel=0&showinfo=0>

Fig. 4A.2) ROV video of steep ridges of coalesced hummocky flows draped with elongate pillows on the south, then north rift zones. The andesite flows produced larger diameter, bread-crust textured lava pillows and larger hummocks, but otherwise they resemble the basalt pillows. For scale, the red dots in the center of the frame are lasers 29 cm apart.

Talus slopes surrounding hummocks were constructed during the eruptions, rather than from subsequent faulting (e.g., Clague et al., 2020), as talus that fell from pillows above in recent eruptions attests.

[VIDEO] <https://www.youtube.com/embed/kFjom2iCUIQ?rel=0&fs=1&modestbranding=1&rel=0&showinfo=0>

Fig. 4A.3) ROV video from 2013 of lava pillows that broke during the 2011 eruption to form talus, and even dripped to form "lavacicles".

4B. Deeper on the rift zones are steep cones of high-MgO composition lavas.

Steep cones of primitive, depleted MORB basaltic lavas ($\text{MgO} > 9 \text{ wt\%}$ and $\text{K}_2\text{O}/\text{TiO}_2 < 0.05$; see Panel 5) are first observed on both rift zones at 1800 m depth and 18 km from the caldera. These cones have rugged summits with deep, stellate embayments above smooth slopes of pillow talus, that probably formed during their construction. They are built upon lower-MgO flows. A single sheet flow at the summit has $\text{MgO} > 9 \text{ wt\%}$, but is not a D-MORB like these deep rift cones. These lavas are too primitive to have been emplaced by lateral dikes from the summit reservoir and are inferred to have been fed vertically from the underlying mantle.

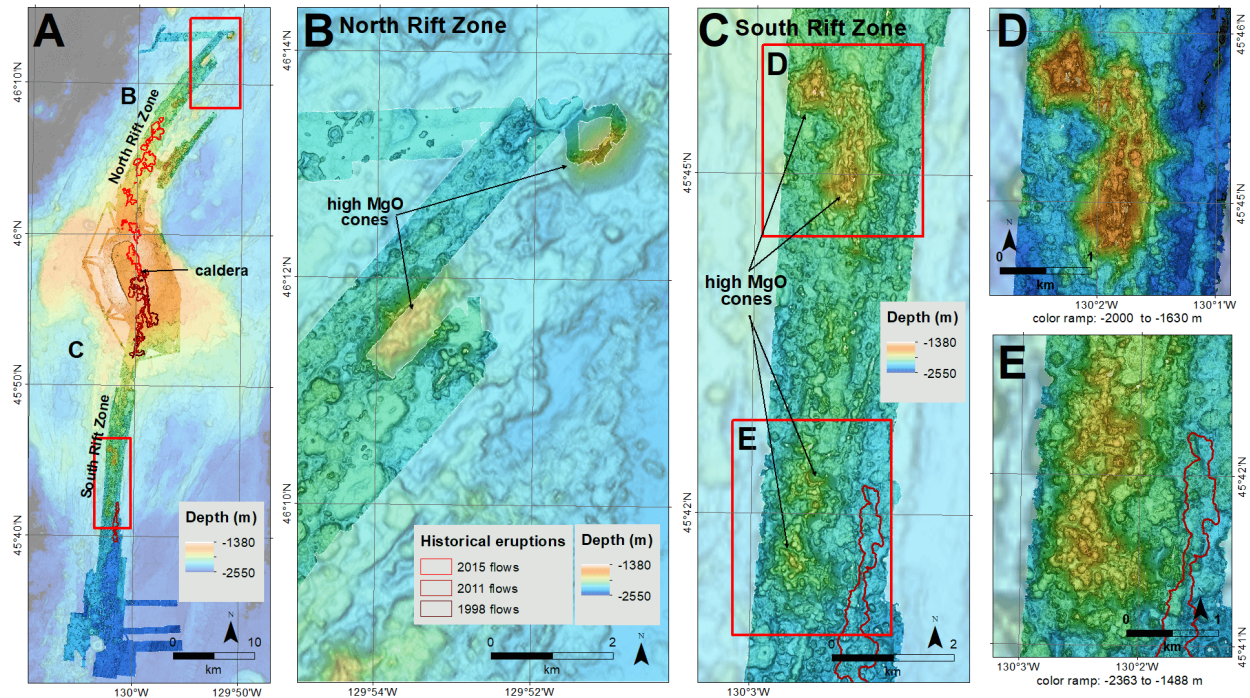


Fig 4B.1) Maps of high-MgO cones deep on the rift zones.

A: Location of maps B-E with known high-MgO cones indicated. Other cones have similar appearance but have not been sampled to ascertain their compositions.

B: North rift zone: Two high-MgO cones have been partially mapped with the AUV.

C: South rift zone: Two high-MgO cones have been mapped with the AUV.

[VIDEO] https://www.youtube.com/embed/otsaH_zM7kk?rel=0&fs=1&modestbranding=1&rel=0&showinfo=0

Fig 4B.2) Video from ROV dive ascending the smooth apron of talus around a high-MgO cone deep on the north rift zone.

4C. Deeper still, emanating from both distal rift axes beginning ~30 km from the caldera, lie voluminous inflated sheet and inflated hummocky flows.

These flows have a combined area of over 150 km^2 . Found throughout their expanses are large collapses typically 30-60 m deep, but up to 100 m deep in the south rift flows and 135 m deep in the north rift flow. The depth of collapses suggests how thick the flows were.

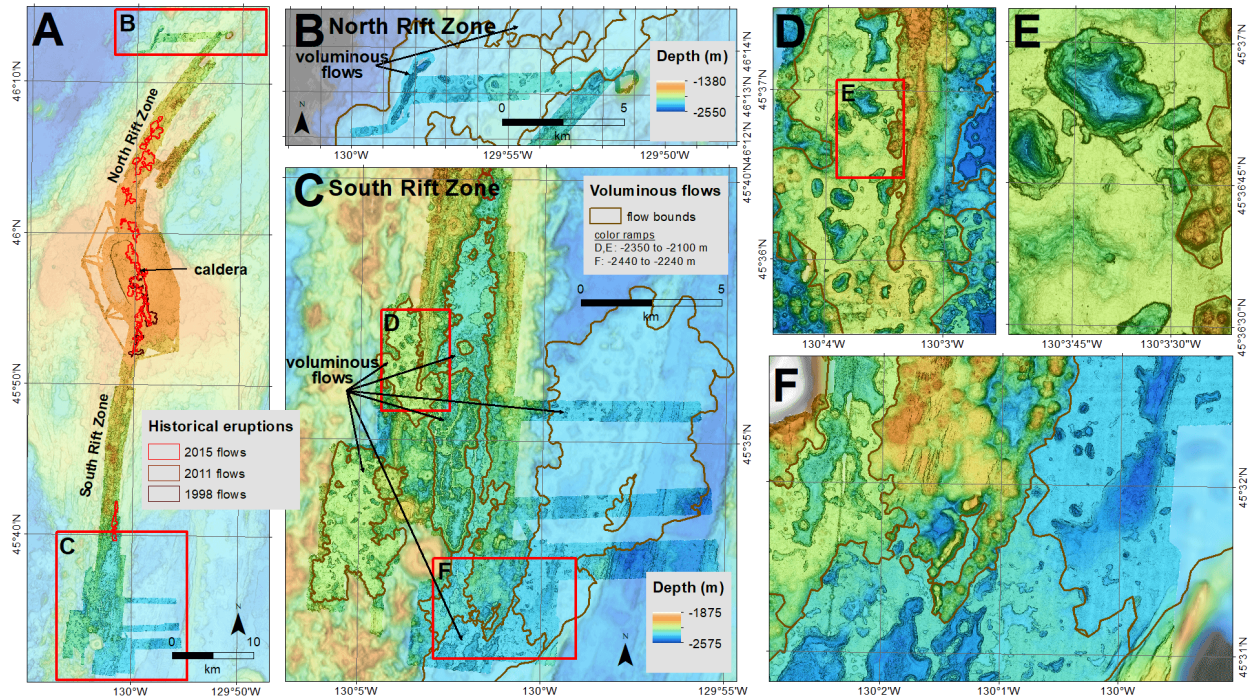


Fig. 4C.1) Maps of voluminous flows on the distal rift zones.

[VIDEO] <https://www.youtube.com/embed/HwuFLq48eV4?rel=0&fs=1&modestbranding=1&rel=0&showinfo=0>

Fig 4C.2) Video from ROV dives on voluminous flows on the distal south rift zone.

The flows on the distal south rift erupted ~1250 years ago and the ones on the north rift ~13,000 years ago, as determined from ^{14}C ages of planktic foraminifera tests that first landed on flows (e.g., Clague et al., 2013). The enormous volumes of these flows are on the order of the volume of the caldera. The emptying of the magma chamber during their eruptions may have caused collapses of the caldera (Clague et al., 2019).

5. FLOW CHEMISTRY AND MORPHOLOGY

MgO content: Flow morphology does not correlate quite as expected with MgO content, which scales with melt temperature. Most of the rift zone lavas fall into a narrow range of basaltic MgO contents (7.0 to 7.7 wt%), yet produced channelized sheet flows to hummocky flows (Panel 3). However, the most mafic basalts (MgO > 9 wt%) constructed steep cones rather than feeding expansive flows (Panel 4B).

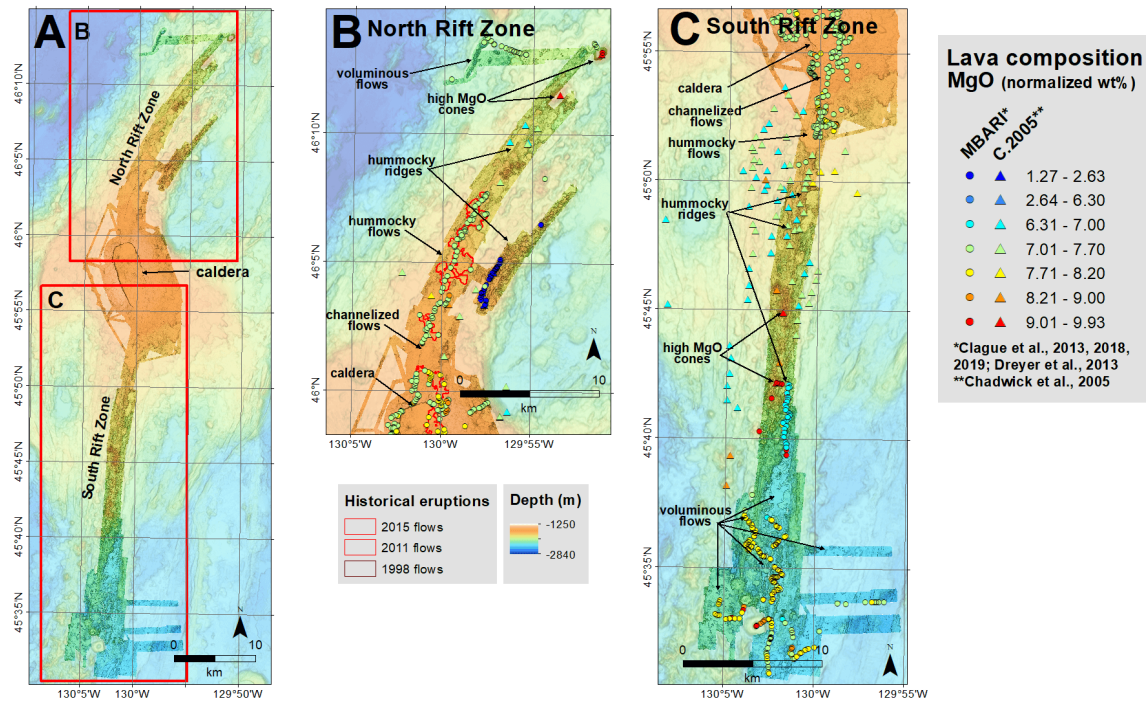


Fig. 5.1) Maps showing lava composition (as MgO weight %) of sampled lavas along the rift zones. Quench temperature scales with MgO content, so higher MgO flows should have lower viscosity (see Clague et al., 2018).

In some ways flows behaved as expected:

- The unusual andesite lava (with MgO of 1.5 to 2.5 wt%, see also poster V040-0019) on the north rift produced hummocky flows with both larger pillows and larger hummocks (Panel 4A) than typical of the basalts.
- The trend toward hummocky flows down-rift in the 1998, 2011, and 2015 eruptions may be explained by cooling during transport within the dikes (melt temperatures decreased ~0.5 to 0.9 °C/km down-rift as determined by decreasing MgO content of the glasses, Clague et al., 2018), and reduced driving pressure with increasing dike length from the summit reservoir (e.g., Grossman-Poneman et al., 2020).
- The voluminous flows (Panel 4C) farther from the caldera are higher MgO (7.7 to 8.2 wt% on the distal south rift, and 7.1 to 7.4 wt% on the distal north rift, Fig. 5.1), which suggests less cooling occurred.

Crystal content: The crystal load does not seem to have impacted flow morphology. Most Axial lavas, over the full range of MgO contents, are aphyric, whether the flows are channelized or hummocky flows or steep cones. The voluminous flows on the distal south rift zone (Panel 4C) are plagioclase ultra-aphyric, and the similar-looking voluminous flows on the north rift are only sparsely plag-phyric.

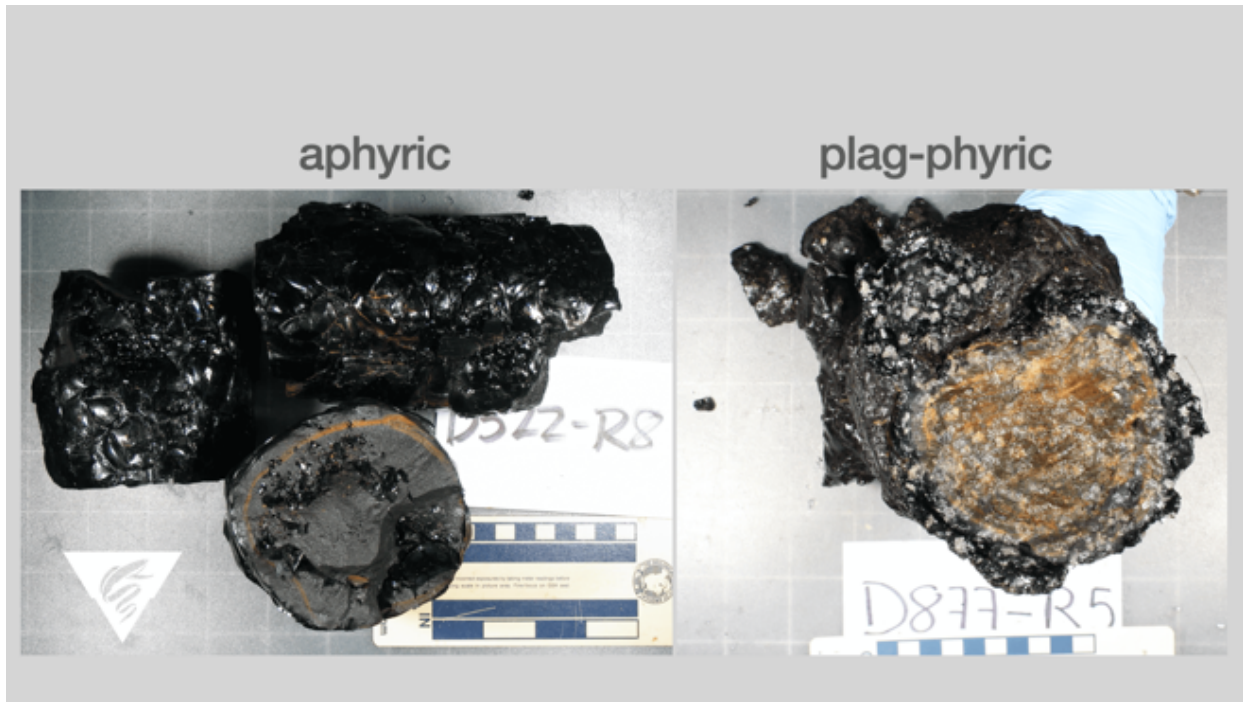


Fig 5.2) Photos of aphyric (crystal-free) and plagioclase-phyric (estimated 15-20% phenocrysts) lava samples. Upper scale is in cm.

6. CONCLUSIONS

The systematic flow morphology variations do not correlate with magma viscosity (Panel 5) or slope (which is nearly constant at 2% down-rift, Panel 2). That leaves dike width as an important control on the eruption rate and therefore of flow morphology along the rift zones, as proposed by Head et al. (1996).

Lateral transport down-rift through long dikes from the summit, as observed in the historical flows, cools the magma and also reduces the driving pressure and eruption rate, so that hummocky flows form down-rift whereas channelized sheet flows erupt up-rift. The voluminous flows on the distal rift zones, especially those of crystal-rich basalt, were likely fed through unusually wide dikes. The near-primary D-MORB lavas of the rare, steep stellate high-MgO cones deep on the rift zones rose vertically through narrow conduits directly from the mantle. Similar depleted melts rising closer than 18 km from the summit are focused into the summit magma reservoir where they hybridize with more enriched Cobb hot-spot influenced melts to form the ubiquitous N- and T-MORBs that characterize the summit and upper rifts at Axial Seamount.

DISCLOSURES

Acknowledgements

We thank Bill Chadwick for his thoughtful feedback. We are grateful to Kris Walz and Kyra Schlining of the MBARI Video Lab for their assistance with producing the videos, and to Hans Thomas and the MBARI AUV Team, the Captains and crews of the R/V *Zephyr* and R/V *Rachel Carson*, the pilots of the ROV *Tiburón* and ROV *Doc Ricketts*, and the Captain and crew of the R/V *Western Flyer* for their professional expertise, dedication, and hard work at sea.

AUTHOR INFORMATION

MBARI Submarine Volcanism Group: <https://www.mbari.org/science/seafloor-processes/volcanoes/>
(<https://www.mbari.org/science/seafloor-processes/volcanoes/>)

MBARI Seafloor Mapping Lab: <https://www.mbari.org/technology/seafloor-mapping/>
(<https://www.mbari.org/technology/seafloor-mapping/>)

Jennifer B. Paduan, Senior Research Specialist

Monterey Bay Aquarium Research Institute (MBARI)

7700 Sandholdt Road, Moss Landing, CA 95039

<https://www.mbari.org/paduan-jennifer/> (<https://www.mbari.org/paduan-jennifer/>)

paje@mbari.org

David A. Clague, Senior Scientist

Monterey Bay Aquarium Research Institute (MBARI)

7700 Sandholdt Road, Moss Landing, CA 95039

<https://www.mbari.org/clague-david/> (<https://www.mbari.org/clague-david/>)

clague@mbari.org

David W. Caress, Principal Engineer

Monterey Bay Aquarium Research Institute (MBARI)

7700 Sandholdt Road, Moss Landing, CA 95039

<https://www.mbari.org/caress-dave/> (<https://www.mbari.org/caress-dave/>)

caress@mbari.org

Morgane Le Saout

GEOMAR Helmholtz Centre for Ocean Research, Kiel, Germany

https://www.researchgate.net/profile/Morgane_Le_Saout (https://www.researchgate.net/profile/Morgane_Le_Saout)

mlesaout@geomar.de

Brian M. Dreyer, Marine Analytical Labs Manager

Institute of Marine Sciences, University of California, Santa Cruz

Santa Cruz, CA 95064

https://www.researchgate.net/profile/Brian_Dreyer (https://www.researchgate.net/profile/Brian_Dreyer)

bdreyer@ucsc.edu

ABSTRACT

Meter-scale AUV mapping of 85-km of the summit and rift zones of Axial Seamount shows systematic variation in morphology of the lava flows with depth and distance from the caldera. ROV sampling reveals flow age and chemistry variations. Each rift zone has a steady downward slope of ~2% outside the caldera. In the caldera and first few km down the rift zones, flows are predominantly channelized sheet flows with collapses along the channels. Mid-rift, drained inflated hummocky flows consisting of complex mounds with tumuli and lava lakes, and narrow ridges of hummocky mounds become common. On the axis of the south rift, the first cones with craters occur 3.2 km from the caldera at 1600 m depth, and broad inflated hummocky flows emplaced through complex lava tubes first appear 6 km down-rift at 1715 m. On the north rift, similar cones and complex flows appear at 10.5 km down-rift at 1725 m depth. The historical flows exemplify this variation: on the upper south rift as channelized sheet flows in 1998 and 2011 erupted from fissures that extended 6.5 km down-rift; on the middle north rift, inflated hummocky flows up to 126 m thick erupted in 2015 from fissures 17.5 km from the caldera; and on the distal south rift, a narrow ridge of coalesced hummocks 160 m tall formed during the 2011 eruption. Older and older lavas remain exposed at greater distances from the more active summit and upper rift zones. Deep on the rift zones, stellate and steep cones with smooth talus slopes occur that did not feed expansive flows, despite being constructed of hotter, less viscous, near-primary magmas. These cones are first observed on both rift zones at 1800 m depth and 18 km from the caldera. Deeper still, emanating from both distal rift axes beginning ~30 km from the caldera, lie voluminous inflated sheet and inflated hummocky flows 30 to 135 m thick with combined area of over 150 km². The plagioclase-phyric voluminous flows on the south rift erupted ~1250 years ago, and the aphyric ones on the north rift ~13,000 years ago. Eruption rate is the most likely cause of the flow morphology changes since estimated magma viscosity does not correlate with flow morphology. Lateral transport through long dikes would slow magma delivery unless dike widths are large. The near-primary magmas may have risen through narrow conduits from the mantle to the distal rifts.

REFERENCES

- Caress, D.W., Clague, D.A., Paduan, J.B., Martin, J.F., Dreyer, B.M., Chadwick Jr, W.W., Denny, A., & Kelley, D.S. (2012). Repeat bathymetric surveys at 1-metre resolution of lava flows erupted at Axial Seamount in April 2011. *Nature Geoscience*, 5(7): 483-488. doi: 10.1038/NGEO1496.
- Chadwick, J., Perfit, M., Ridley, I., Jonasson, I., Kamenov, G., Chadwick, W., Embley, R., le Roux, P., & Smith, M. (2005), Magmatic effects of the Cobb hot spot on the Juan de Fuca Ridge, *J. Geophys. Res.*, 110, B03101, doi:10.1029/2003JB002767.
- Chadwick, W.W., Clague, D.A., Embley, R.W., Perfit, M.R., Butterfield, D.A., Caress, D.W., Paduan, J.B., Martin, J.F., Sasnett, P., Merle, S.G., & Bobbitt, A.M. (2013). The 1998 eruption of Axial Seamount: New insights on submarine lava flow emplacement from high-resolution mapping. *Geochemistry, Geophysics, Geosystems*, 14(10), 3939-3968. doi: 10.1002/ggge.20202.
- Chadwick, W. W., Paduan, J. B., Clague, D. A., Dreyer, B. M., Merle, S. G., Bobbitt, A. M., Caress, D.W., Philip, C.T., Kelley, D. S., & Nooner, S. L. (2016). Voluminous eruption from a zoned magma body after an increase in supply rate at Axial Seamount. *Geophysical Research Letters*, 43(23), 12,063-12,070. <https://doi.org/10.1002/2016GL071327>.
- Clague, D.A., Dreyer, B.M., Paduan, J.B., Martin, J.F., Chadwick, W.W., Caress, D.W., Portner, R.A., Guilderson, T.P., McGann, M.L., Thomas, H., Butterfield, D.A., & Embley, R.W. (2013) Geologic history of the summit of Axial Seamount, Juan de Fuca Ridge. *Geochemistry, Geophysics, Geosystems*, 14(10), 4403-4443. doi: 10.1002/ggge.20240.
- Clague, D.A., Martin, J.F., Paduan, J.B., Butterfield, D.A., Jamieson, J.W., Le Saout, M., et al. (2020). Hydrothermal chimney distribution on the Endeavour Segment, Juan de Fuca Ridge. *Geochemistry, Geophysics, Geosystems*, 21, e2020GC008917. doi: 10.1029/2020GC008917.
- Clague, D.A., Paduan, J.B., Caress, D.W., Chadwick Jr., W.W., Le Saout, M., Dreyer, B.M., & Portner, R.A. (2017) High-resolution AUV mapping and targeted ROV observations of three historic lava flows at Axial Seamount. *Oceanography* 30(4):82–99, <https://doi.org/10.5670/oceanog.2017.426>
- Clague, D.A., Paduan, J.B., Dreyer, B.M., Chadwick, W.W. Jr., Rubin, K.R., Perfit, M.R., & Fundis, A.T. (2018). Chemical variations in the 1998, 2011, and 2015 lava flows from Axial Seamount, Juan de Fuca Ridge: cooling during ascent, lateral transport, and flow. *Geochemistry, Geophysics, Geosystems*, 19(9), 2915-2933. doi: 10.1029/2018GC007708.
- Clague D.A., Portner, R.A., Paduan, J.B., Le Saout, M., & Dreyer, B.M. (2019) Formation of the summit caldera at Axial Seamount. Abstract V43C-0217 presented at 2019 Fall Meeting, AGU, San Francisco, CA.
- Dreyer, B.M., Clague, D.A., & Gill, J.B. (2013), Petrological variability of recent magmatism at the Axial Seamount Summit, Juan de Fuca Ridge, *Geochemistry, Geophysics, Geosystems*, 14, 4306– 4333, doi:10.1002/ggge.20239.
- Grossman-Ponemon, B.E., Heimisson, E.R., Lew, A.J., & Segall, P. (2020) Logarithmic growth of dikes from a depressurizing magma chamber, *Geophys. Res. Lett.*, 47, doi:10.1029/2019GL086230.
- Head, J.W., Wilson, L., & Smith, D.K. (1996), Mid-ocean ridge eruptive vent morphology and substructure: Evidence for dike widths, eruption rates, and evolution of eruptions and axial volcanic ridges, *J. Geophys. Res.*, 101(B12), 28265– 28280, doi:10.1029/96JB02275.
- Le Saout, M., Bohnenstiehl, D.R., Paduan, J.B., & Clague, D.A. (2020) Quantification of eruption dynamics on the north rift at Axial Seamount, Juan de Fuca Ridge. *Geochemistry, Geophysics, Geosystems*, 21, e2020GC009136. doi: <https://doi.org/10.1029/2020GC009136>.

Yeo, I.A., Clague, D.A., Martin, J.F., Paduan, J.B., & Caress, D.W. (2013). Pre-eruptive flow focussing in dikes feeding historical pillow ridges on the Juan de Fuca and Gorda Ridges. *Geochemistry, Geophysics, Geosystems*, 14(9), 3586-3599. doi: 10.1002/ggge.20210.